RESEARCH PAPER

Tailoring the Electronic and Optical Properties of PVA/SeO$_2$/SiC Nanostructures for Electronics Devices

Safa Zuhair Hussein* , and Hind Ahmed

University of Babylon, College of Education for Pure Sciences, Department of Physics, Iraq

ARTICLE INFO

ABSTRACT

This work aims to investigate the structure, electronic and optical properties of PVA/SeO$_2$/SiC nanostructures to employ in various electronic devices. Density functional method was applied using Gaussian 09 software and Gauss view 5.0 program. Analysis of (PVA-SeO$_2$-SiC) (90Atom) nanacomposites were done at B3LYP level by using LanL2DZ level of DFT (Density Functional Theory). Synthesized of (PVA-SeO$_2$-SiC) (90Atom) nanacomposites were characterized by UV–visible, FT-IR, proton NMR spectroscopes. Nanacomposites were designed and calculated for different properties, absorption spectra, dipole moment and frontier molecular orbitals, by calculating the HOMO/LUMO energy orbitals via density functional theory method. The final results indicated to the PVA/SeO$_2$/SiC nanostructures may be useful in different electronics and optics fields.

INTRODUCTION

Selenium is one of the greatest significant and fascinating trace elements in the field of health in addition to human biology [1]. The properties of bulk selenium are to a large extent determined by Sen allotropes and aggregates. As a consequence, semiconducting selenium nanomaterials have great potential in electronics [2]. Selenium is the single element that has codon in messenger RNA which make probable its insertion into the Seleno protein in the form of seleno-cysteine[3].Carbides of transition metals form an interesting class of materials in which anions and cations are held together by a mixture of strong ionic, covalent, and metallic bonds [4].Gaussian 03 program (computer software which is capable of predicting many properties of molecules and reactions, including the molecular energies and structures)

[5] to make the calculation. The present work aims to design of PVA/SeO$_2$/SiC nanostructures to use in various electronic devices.

THEORETICAL PART

Energy gap refers to energy difference between the highest occupied molecular orbital (HOMO) and lowest unoccupied molecular orbital (LUMO) according to the Koopmans theorem [5]:

$$E_{gap} = E_{LUMO} - E_{HOMO} \qquad (1)$$

Here E$_{gap}$ indicates the energy gap E$_{LUMO}$, and E$_{HOMO}$ denoted the energies of HOMO and LUMO in consecution.

Ionization Potential energy (IP) is defined as the minimum energy required to remove an electron from the atom in a gaseous phase. Ionization

* *Corresponding Author Email: mastersumer@yahoo.com*

energy is expressed in units of electron Volt (eV) [6].

$$I_E = -E_{HOMO} \qquad (2)$$

Electron affinity can be defined as the energy released upon attachment of an electron to an atom or molecule resulting in the formation of the negative ion [5].

$$E_A = -E_{LUMO} \qquad (3)$$

One of the global quantities is chemical potential (μ); it measures the escaping tendency of an electronic cloud. is related to two known quantities, I_E and E_A, as in the following relationship [7].

$$\mu \approx \frac{1}{2}(E_{HOMO} + E_{LUMO}) \approx -\frac{1}{2}(I_E + E_A) \qquad (4)$$

Chemical hardness is the resistance of a species to lose electrons, for insulator and semiconductor, hardness is half of the energy gap. we can calculate

the chemical hardness (H) [8]:

$$H = \frac{I_E - E_A}{2} \qquad (5)$$

Chemical softness is the inverse with hardness as below equation [9]:

$$S = \frac{1}{2H} \qquad (6)$$

Electrophilicity can be defined as a measure of energy lowering due to maximal electron flow between donor and acceptor [10]:

$$\omega = \frac{\mu^2}{2H} \qquad (7)$$

R. Mulliken defined electronegativity as the average of the ionization energy and electron affinity as follows [9]:

$$E_N = \frac{1}{2}(I_E + E_A) \qquad (8)$$
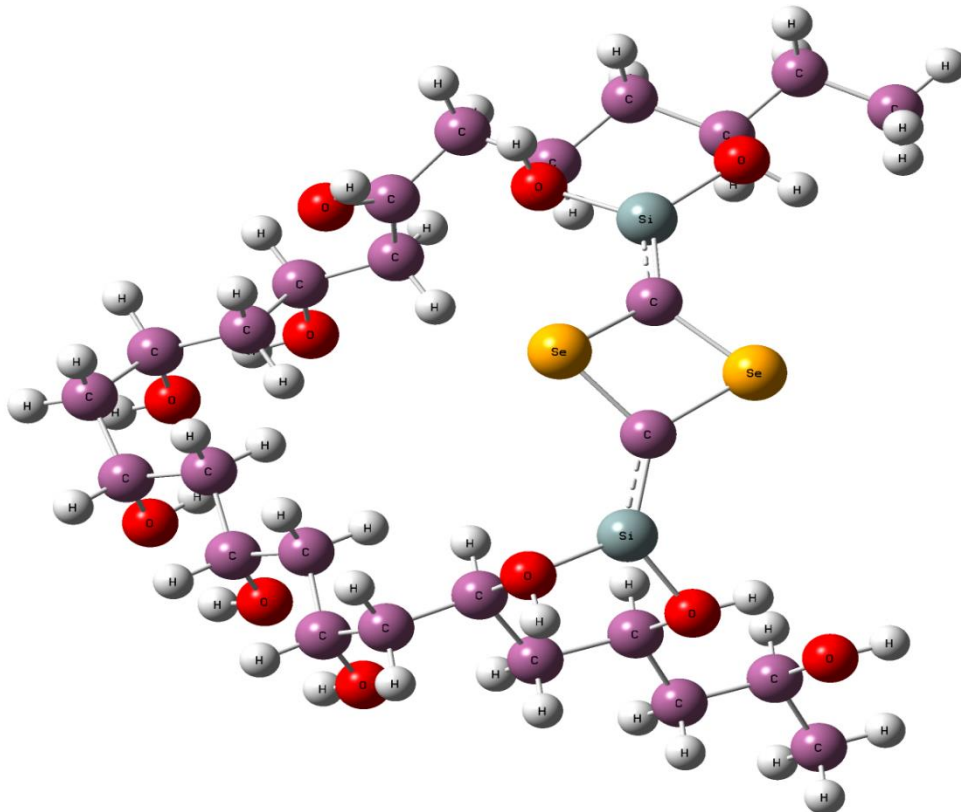
The electric dipole polarizability is the measure

Fig. 1. Optimize the geometriesof (PVA-SeO₂-SiC)(90Atom).

of the linear response of the electron density in the presence of an infinitesimal electric field F and it represents a second order variation in energy. The polarizability is calculated as the main value as given in the following equation [11,12].

$$< \alpha >= \frac{1}{3} (\alpha_{xx} + \alpha_{yy} + \alpha_{zz}) \qquad (9)$$

RESULTS AND DISCUSSION

Fig. 1 shows find the relaxation of the molecule, in which the optimized structure of the molecule is the structure at minimum energy, and it is performed by finding the first derivative of the energy with respect to distance between different atoms. Table 1 represents the standard orientation of all atoms in the molecule. The bonds values
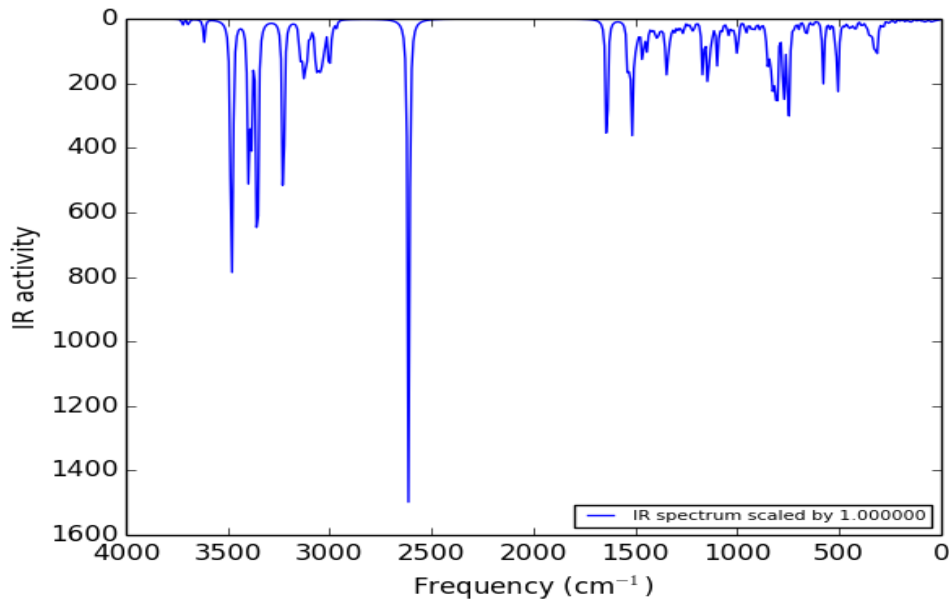

Fig. 2. IR spectra of ((PVA-SeO₂-SiC) (90Atom) composites.

Table 1. Average lengths of bond in (Å) and the angles in degree

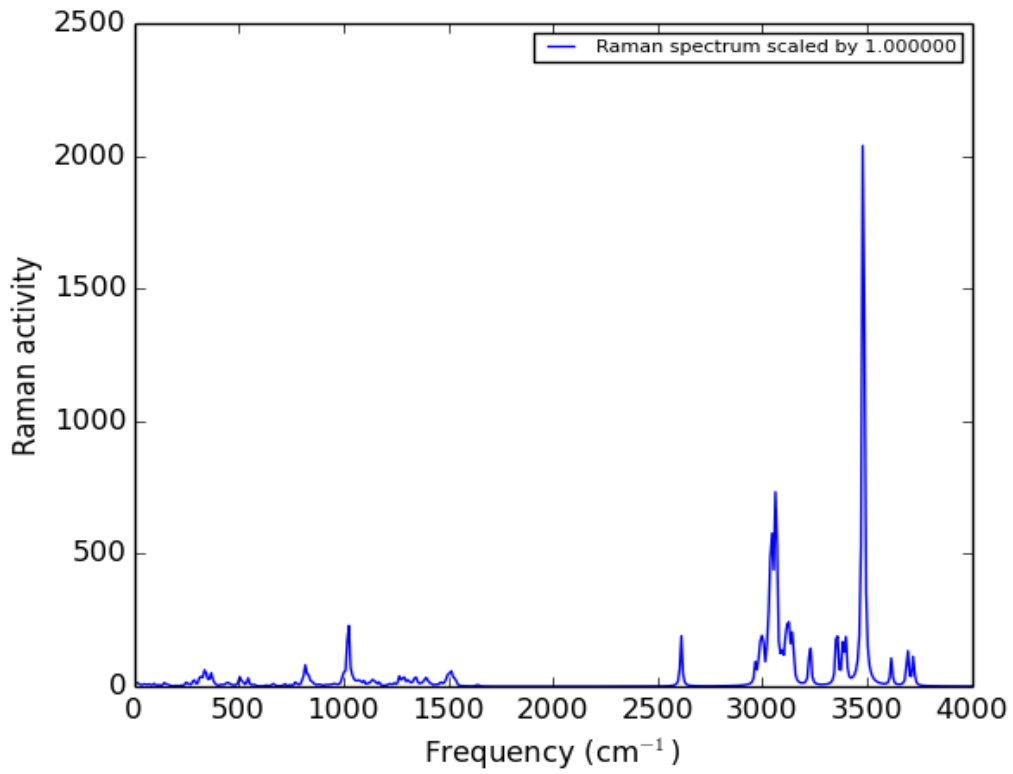| Measurements	The optimization parameters	Values
Bonds Å	(C-C)	1.534
	(C-O)	1.515
	(C-H)	1.096
	(O-H)	0.977
	(O-Se)	1.931
	(Se-C)	1.962
	(Si- C)	1.799
Angles Deg.	(C-C-C)	113.585
	(C-O-H)	109.555
	(Se-C -Se)	97.740
	(O-Si-C)	95.580

Fig. 3. Raman intensities of (PVA-SeO$_2$-SiC)(90Atom) composites with vibration frequency .
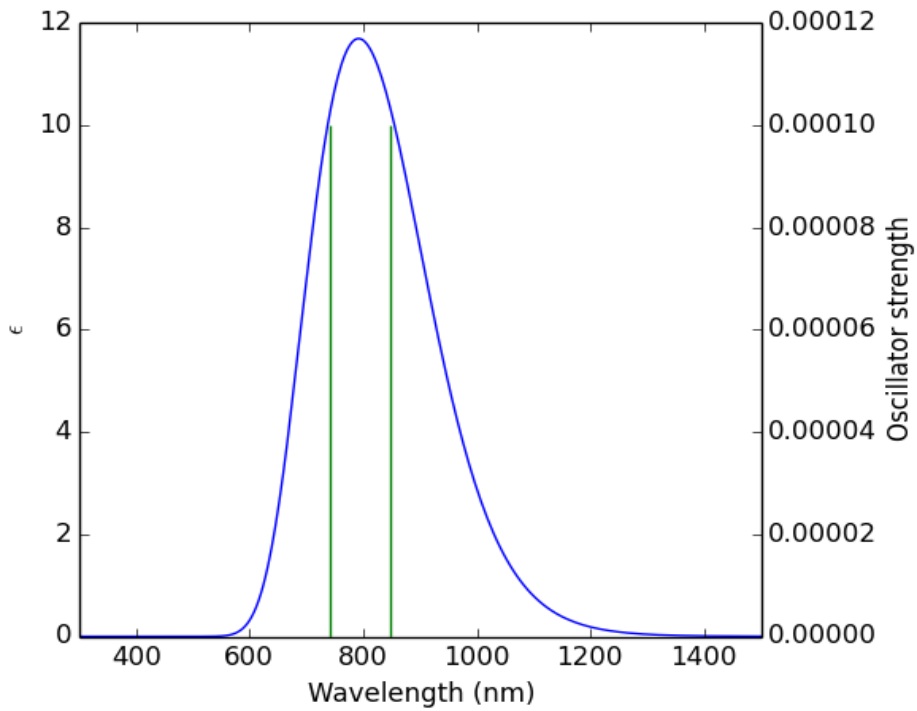

Fig. 4. UV-Vis spectrum for (PVA-SeO$_2$-SiC) (90Atom) composites.

in present work are in a well agreement with previous theoretically studies [2,13,14].

Fig. 2 shows the IR-Spectrum of (PVA-SeO$_2$-SiC)

(90Atom)composites using DFT.It has been found that the strong peak observed at (2800cm^{-1}) is attributed to the (O-H) groups.
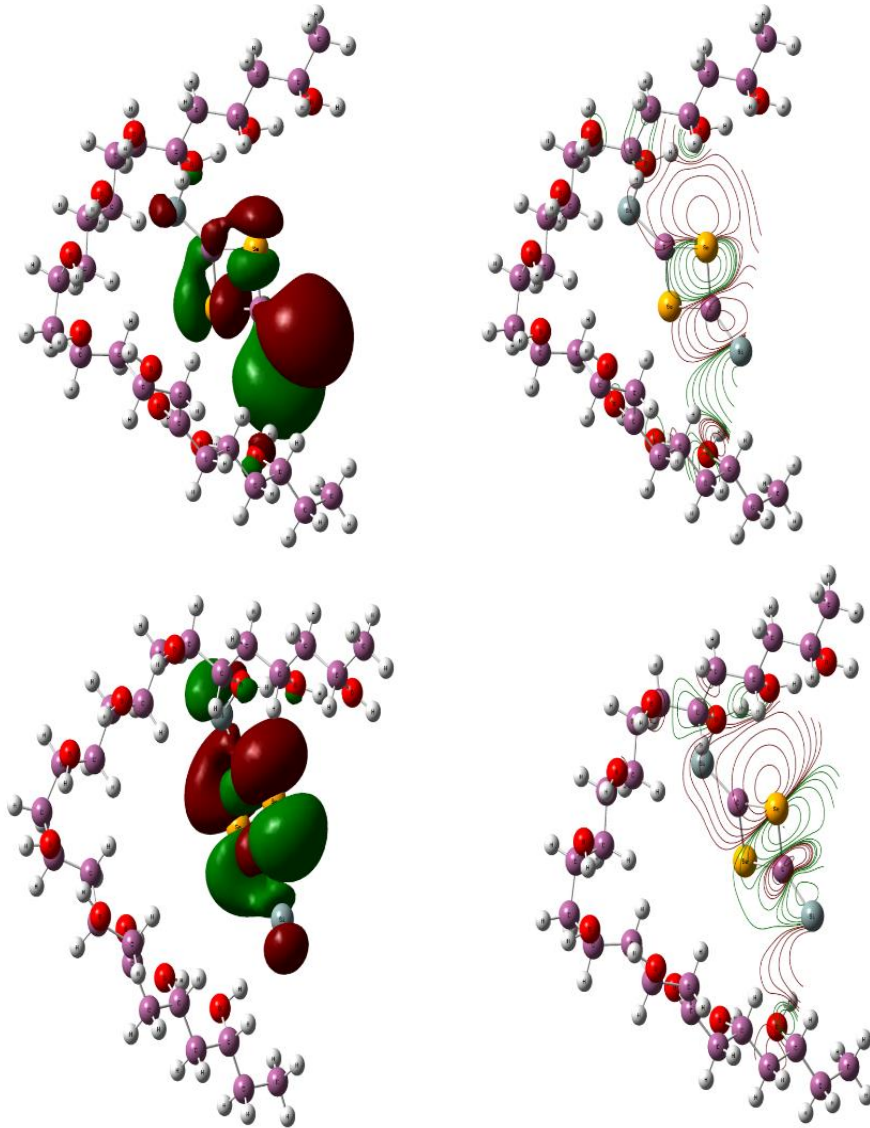

Fig. 5. The distribution of HOMO (up) and LUMO (down) (PVA-SeO$_2$-SiC) (90Atom) composites

Table 2. Energy gap values of in (eV) of structures

(PVA-SeO$_2$-SiC)(90Atom)composites		
E$_{HOMO}$ (eV)	E$_{LUMO}$ (eV)	E$_g$ (eV)
-6.057	-4.209	1.848

In Raman spectroscopy, a change is experiential in the polarization of molecules; that is, a visible or ultraviolet photons interacts with the vibrating molecular bonds, gaining or losing part of their energy, thereby generating the spectrum [15]. Fig. 3 shows the Raman spectra of (PVA-SeO$_2$-SiC) (90Atom) composites. Strengths of Raman spectra

depend on the probability that photon with particular wavelength will be absorbed.

Fig. 4 show the UV-Vis spectra Visible and Ultra Violet spectrum is dependent on upon the electronics structure of the molecule. The UV-Vis calculations of the (PVA-SeO$_2$-SiC) (90Atom) composites studied from the B3LYP-TD/
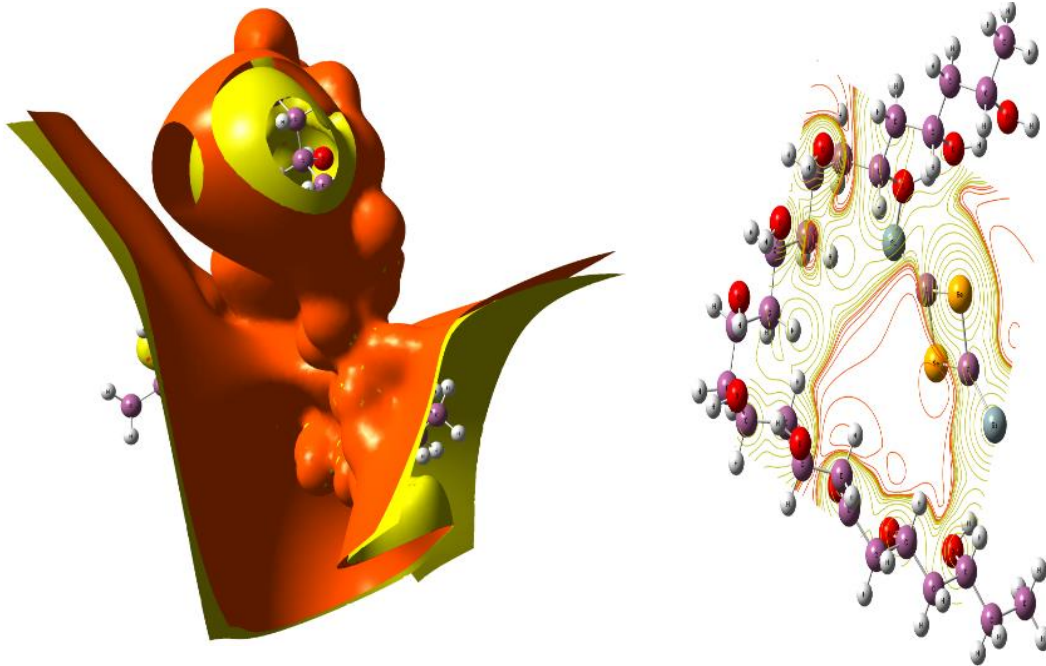

Fig. 6. Electrostatic potential distribution surface for(PVA-SeO$_2$-SiC)(90Atom).

Table 3. Electronic properties values in eV of the structure.

Property	(PVA-SeO$_2$-SiC)(90Atom)composites
Total energy	-1873.535(a.u)
Ionization potential	6.857
Electron affinity	4.209
Electronegativity	5.533
Chemical hardness	1.324
Chemical softness	0.377
Chemical potential	-5.533
Electrophilicity	11.561
Dipole moment (Debye)	7.228

Table 4. The calculated α_{ave} and it is components of (PVA-SeO$_2$-SiC) (90Atom) composites.

Polarizability (a.u)			
α_{xx}(a.u)	α_{yy}(a.u)	α_{zz}(a.u)	α_{ave}(a.u)
466.269	510.338	399.152	458.586

LanL2DZ method included the excitation energy, wavelength, oscillator strength and electronic transition.

Table 2 represents the energy gap of (PVA-SeO$_2$-SiC) (90Atom) composites and compared with the experimental data in Ref [16,14]. Fig. 5 illustrates the 3-D distribution of HOMO^s and LUMO^s for the studied structures. The visualization of HOMO − LUMO obviously characterizes the electron cloud in occupied and virtual orbital. The green color cloud shows the HOMO and red color shows the LUMO electrons in SeO$_2$ nanostructures. DOS spectrum, the charge density is low in occupied orbital and high in virtual orbital for pure, O and H substituted SeO$_2$ nanostructures. This mentions the localization of charges along the virtual orbitals than in occupied orbitals.

Fig. 6 illustrates the electrostatic surfaces potential (ESP) distribution of structures calculated from the total self-consistent field SCF. ESP distributions of structure are caused by repulsive forces or by attracting regions around each structure. In general, the ESP surfaces of (PVA-SeO$_2$-SiC) (90Atom) composites are dragged toward the negative charges positions in the each

molecule bases the high electronegativity oxygen atoms [3.5 eV].

Table 3 shows the results of the ground state energy ET in a. u and some electronic properties of (PVA-SeO$_2$-SiC) (90Atom) composites calculated at the same level of theory. These properties are included the ionization energy IE, electron affinity EA, electronegativity , electrochemical hardness H and electrophilic index ω [16].

Table 4 shows the average Polarizability α$_{ave}$ and it is components in a.u of (PVA-SeO$_2$-SiC) (90Atom) composites.

The density of states of (PVA-SeO$_2$-SiC) (90Atom) composites as a function of energy levels were calculated by using the DFT-B3LYP/LanL2DZ level of theory. Fig. 7 shows the degenerate states as a function of energy levels for the studied structure, this degeneracy produced by the existence of the new types of atoms, and that leads to changing the bond lengths and angles or changing the geometry of the structure.

The gauge-including atomic orbitals (GIAO) method issued to calculate the absolute shielding constants (in ppm) of (PVA-SeO$_2$-SiC) (90Atom). Calculation gave the calculated 1H chemical shifts
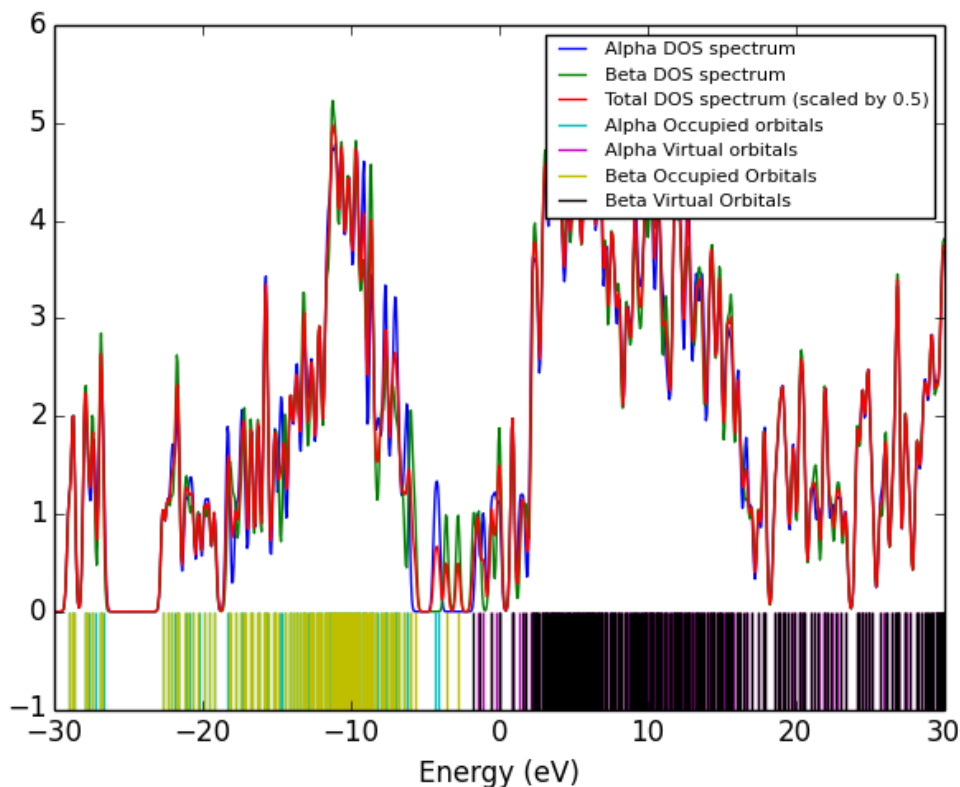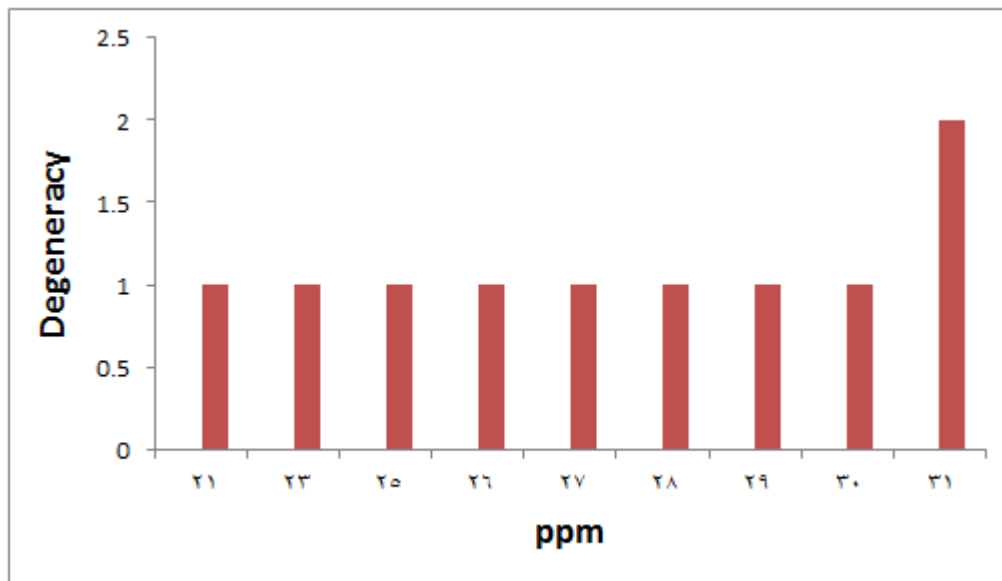

Fig. 7. DOS of (PVA-SeO$_2$-SiC) (90Atom) composites.

Fig. 8. Nuclear Magnetic Resonance of (PVA-SeO$_2$-SiC) (90Atom).

(in ppm) of structures. Fig. 8 1H NMR spectra of (PVA-SeO$_2$-SiC) (90Atom) and compared with the experimental data in Ref [17].

CONCLUSION

In this paper, design, structural, optical and electronic properties of PVA/SeO$_2$/SiC nanostructures to use in different electronics fields. Good relax of the (PVA-SeO$_2$-SiC) (90Atom) was obtained by B3LYP-DFT at Gaussian 09 package of program and agree with that relax done by using the LanL2DZ. With high resolution methods, which made it possible to separate 1H NMR spectrum of (PVA-SeO$_2$-SiC) (90Atom) structure, interactions were characterized by 1H NMR chemical shifts of SeO$_2$. The results indicated to the PVA-SeO$_2$-SiC (90Atom) structures have good optical and electronic properties with low energy band gap (2.648eV) which make it appropriate for many applications.

CONFLICT OF INTEREST

The authors declare that there is no conflict of interests regarding the publication of this manuscript.

REFERENCES

1. Rybínová M, Červený V, Hraníček J, Rychlovský P. UV-photochemical vapor generation with quartz furnace atomic absorption spectrometry for simple and sensitive determination of selenium in dietary supplements. Microchem J. 2016;124:584-593.
2. Sarkar J, Dey P, Saha S, Acharya K. Mycosynthesis of selenium nanoparticles. Micro & Nano Letters. 2011;6(8):599.
3. Srivastava N, Mukhopadhyay M. Biosynthesis and Structural Characterization of Selenium Nanoparticles Using Gliocladium roseum. J Cluster Sci. 2015;26(5):1473-1482.
4. Hashim A, Abduljalil H, Ahmed H. Analysis of Optical, Electronic and Spectroscopic properties of (Biopolymer-SiC) Nanocomposites For Electronics Applications. Egyptian Journal of Chemistry. 2019;0(0):0-0.
5. Park S, Kampen TU, Zahn DRT, Braun W. Energy level alignment driven by electron affinity difference at 3,4,9,10-perylenetetracarboxylic dianhydride/n-GaAs(100) interfaces. Appl Phys Lett. 2001;79(25):4124-4126.
6. Sadasivam K, Kumaresan R. Theoretical investigation on the antioxidant behavior of chrysoeriol and hispidulin flavonoid compounds – A DFT study. Computational and Theoretical Chemistry. 2011;963(1):227-235.
7. Gece G. Theoretical evaluation of the inhibition properties of two thiophene derivatives on corrosion of carbon steel in acidic media. Mater Corros. 2012;64(10):940-944.
8. Atkins P, Friedman R, editors. Molecular Quantum Mechanics: Oxford University Press; 2010.
9. Karelson M. Quantum-Chemical Descriptors in QSAR. Computational Medicinal Chemistry for Drug Discovery: CRC Press; 2003.
10. Shenghua L, He Y, Yuansheng J. Lubrication Chemistry Viewed from DFT-Based Concepts and Electronic Structural Principles. Int J Mol Sci. 2003;5(1):13-34.
11. Camargo AJ, Honório KM, Mercadante R, Molfetta FA, Alves CN, Silva ABFd. A study of neolignan compounds with biological activity against Paracoccidioides brasiliensis by using quantum chemical and chemometric methods. J Braz Chem Soc. 2003;14(5):809-814.
12. Udhayakala P, Jayanthi A, Rajendiran TV, Gunasekaran

S. Quantum chemical studies on some thiadiazolines as corrosion inhibitors for mild steel in acidic medium. Res Chem Intermed. 2012;39(3):895-906.

13. Rybakov VB, Aslanov LA, Volkov SV, Grafov AV, Pekhn'o VI, Fokina ZA. Crystal and molecular structures of the binuclear complex of rhodium(III) chloride with selenium dichloride and the complex of iridium(III) chloride with sulfur dichloride and tetrachloride. J Struct Chem. 1992;33(3):460-463.

14. Wentz KE, Molino A, Freeman LA, Dickie DA, Wilson DJD, Gilliard RJ. Reactions of 9-Carbene-9-Borafluorene Monoanion and Selenium: Synthesis of Boryl-Substituted Selenides and Diselenides. Inorganic Chemistry. 2021;60(18):13941-13949.

15. Carter ED. Mapping Latin America: A Cartographic Reader. Jordana Dym and Karl Offen, eds. Chicago: University of Chicago Press, 2011. xx and 338 pp.; maps, ills., notes, bibliog., index. $39.00 paper (ISBN 978-0-226-618210); $134.00 cloth (ISBN 978-0-226-618227); $31.00 electronic (ISBN 978-0-226-921815). The AAG Review of Books. 2013;1(1):45-49.

16. Yaqoob M, Gul S, Zubair NF, Iqbal J, Iqbal MA. Theoretical calculation of selenium N-heterocyclic carbene compounds through DFT studies: Synthesis, characterization and biological potential. J Mol Struct. 2020;1204:127462.

17. Santi C, Incipini L, Rongoni E, Bagnoli L, Marini F. New Chiral Electrophilic Selenium Reagents: Synthesis and Structural Investigation. Proceedings of The 16th International Electronic Conference on Synthetic Organic Chemistry; 2012/10/30: MDPI; 2012. p. 1013.